



HAL
open science

Glenohumeral joint and muscles functions during a lifting task

Najoua Assila, Sonia Duprey, Mickaël Begon

► **To cite this version:**

Najoua Assila, Sonia Duprey, Mickaël Begon. Glenohumeral joint and muscles functions during a lifting task. Journal of Biomechanics, 2021, 126, 27p. <10.1016/j.jbiomech.2021.110641>. <hal-03322615>

HAL Id: hal-03322615

<https://hal.science/hal-03322615v1>

Submitted on 19 Aug 2021

HAL is a multi-disciplinary open access archive for the deposit and dissemination of scientific research documents, whether they are published or not. The documents may come from teaching and research institutions in France or abroad, or from public or private research centers.

L'archive ouverte pluridisciplinaire **HAL**, est destinée au dépôt et à la diffusion de documents scientifiques de niveau recherche, publiés ou non, émanant des établissements d'enseignement et de recherche français ou étrangers, des laboratoires publics ou privés.



HAL Authorization

Glenohumeral joint and muscles functions during a lifting task

Najoua Assila^{1,2,3}, Sonia Duprey¹, Mickaël Begon^{2,3}

¹Univ Lyon, Université Claude Bernard Lyon 1, Univ Gustave Eiffel, IFSTTAR, LBMC
UMR_T9406, F69622, Lyon, France

²School of Kinesiology and Exercise Science, Faculty of Medicine, University of Montreal,
QC, Canada

³Sainte-Justine Hospital Research Centre, Montreal, QC, Canada

Submitted as an original article to the *Journal of Biomechanics*

Word count 3707

Address for correspondence:

Najoua Assila
School of Kinesiology and Exercise Science
Faculty of Medicine, University of Montreal
1700 rue Jacques-Tétreault,
Laval, QC H7N 0B6, Canada
Phone: +1 514 343 6111 (45172)
Email: najoua.assila@umontreal.ca

Key words: shoulder; rotator cuff; glenohumeral joint; muscle function; joint function

ABSTRACT

The mobility of the healthy shoulder depends on complex interactions between the muscles spanning its glenohumeral joint. These interactions ensure the stability of this joint. While previous studies emphasized the complexity of the glenohumeral stability, it is still not clear how the kinematics and muscles interact and adapt to ensure a healthy function of the glenohumeral joint. To understand the function of each muscle and degree of freedom of the glenohumeral joint in executing an above-the shoulder box handling task while ensuring stability, we adapted an index-based approach previously used to characterize the lower limb joint and muscle function during locomotion. Forty participants lifted two loads (6 Vs. 12 kg) from hip to eye level. We computed the glenohumeral degrees of freedom and its spanning muscles mechanical powers. We characterized the function of muscles and degrees of freedom using the function indices. The function of the glenohumeral joint underlined its compliancy and design for a large range of motion, while the rotator cuff indices emphasized their stabilizing function. The overall muscle functions underlined the complexity of the glenohumeral stability that goes beyond the rotator cuff. Additionally, the load increase was compensated with changes in the degrees of freedom and muscle functions that seem to favor joint stability. The implemented approach represents a synthesized tool that could quantify the glenohumeral joint and muscles behavior during tridimensional upper limb tasks, which might offer additional insight into motor control strategies, functional alterations related to pathologies or adaptations to external parameters (e.g., load).

1 INTRODUCTION

2 The upper limb is regularly recruited in daily activities. However, due to its neuro-
3 musculoskeletal complexity, the understanding of its functional anatomy is still limited. With
4 the evolution of the erect posture in humans, the upper limb evolved to ensure dexterous
5 manipulation over a wide range of motion. Nevertheless, the upper limb is often recruited for
6 load bearing activities, particularly during occupational handling tasks. The shoulder healthy
7 function, particularly that of its glenohumeral joint depends on intricate interactions between
8 its various muscles (Inman et al., 1996). In order, for shoulder muscles, to actuate and actively
9 stabilize the glenohumeral joint throughout its large range of motion, they have long fascicle
10 lengths, such that their working range remains within the force-length curve middle section
11 (Veeger and van der Helm, 2007). While classical biomechanical approaches predict
12 coordinates and moments of each joint degrees of freedom (DOF), as well as muscle
13 activation and lengths, it is difficult to use their results to draw conclusions on the upper limb
14 joint and muscle behaviors during a handling task. Indeed, the variation of muscle force
15 directions and moment arms during three-dimensional tasks hinders the identification of a
16 sole muscle function. Additionally, while muscle behavior is strongly dependent on the force-
17 length and force-velocity curves (Lappin et al., 2006; Richardson et al., 2005), using these
18 curves to infer muscle functions during a dynamic task remains difficult due to their complex
19 interactions. As muscle architectural features have an impact on its behavior, and thus on the
20 joint function (Biewener, 2016), an approach that synthesizes muscle forces and length
21 change is expected to shed a light on the upper limb function. According to Dickinson et al.
22 (2000), muscle function can be split into four categories: strut, spring, motor and damper. A
23 strut function expresses the capacity to generate large muscle forces (or joint moments) with
24 little change in muscle length (or joint angle). Such behavior would be beneficial for rotator
25 cuff muscles, particularly for their stabilizing action but not for joints with large range of

26 motion. A spring-like behavior expresses the capacity of a structure to store and release elastic
27 energy; a motor-like behavior characterizes a structure that generates positive energy; while a
28 damper-like behavior characterizes a structure that relies on muscle contraction to absorb
29 energy. These four behaviors have been quantified through indices calculated using
30 mechanical energy. While initially introduced for muscles, these categories have also been
31 extrapolated to describe joint behavior. Indeed, this approach successfully identified lower
32 limb joints and muscles functions during walking and running (Lai et al., 2019; Qiao and
33 Jindrich, 2016). Implementing such approach to study the glenohumeral joint would shed a
34 light on the upper limb motor strategies. However, as the healthy function of this joint relies
35 on muscle co-contraction, predicting muscle forces that express the coactivation of muscles is
36 critical to predict their function.

37 Our previous work on the effect of sex and load on the biomechanics of a lifting task
38 presented the complexity of the upper limb biomechanics, as well as the interactions of the
39 various biomechanical variables for a relatively straightforward lifting task (Bouffard et al.,
40 2019; Martinez et al., 2020, 2019). While sex-load interactions were found for joint
41 kinematics (differences linked to the load lifted by women), no sex-load interactions were
42 observed for muscles' activations estimated using musculoskeletal models, nor for their
43 electromyographic signals (EMG). Additionally, no load effect was observed for the relative
44 time spent beyond a critical shear-compression dislocation ratio for the glenohumeral joint
45 reaction force of all participants, despite the increased muscle activation. Local adaptations
46 within the glenohumeral joint could explain the disparity of these results. Indeed, for pointing
47 tasks, shoulder fatigue was reported to induce differences in the shoulder kinematics and in
48 those of the trunk and elbow (Yang et al., 2019). Accordingly, an analysis of the adaptations
49 within the glenohumeral DOF and muscle functions could explain why no changes are

50 observed for muscle activations and why seemingly the load does not impact the
51 glenohumeral risk of dislocation.

52 The objective of this study is to further understand the glenohumeral joint and its muscles
53 functions using an energy index-based approach during a lifting task. It was hypothesized
54 from observation of the shoulder structure and function (multiple joints with scapulohumeral
55 rhythm, large mobility range and muscles with long fascicles) that this approach should yield
56 a minimal strut behavior for the glenohumeral joint DOFs irrespective of sex and load. On the
57 other hand, scapulohumeral muscles, particularly the rotator cuff muscles that act as
58 stabilizers, should mainly have a strut behavior. A secondary objective of this study is to
59 analyze the effect of sex and load on the mechanical power and the predicted behaviors in
60 light of our previous results regarding biomechanical parameters during a lifting task
61 (Bouffard et al., 2019; Martinez et al., 2020, 2019). It is hypothesized that functional
62 adaptations to load within the glenohumeral joint and musculature would occur. Particularly,
63 an increase in the damper-like behavior of joint DOF and muscles is expected to counter the
64 increased risk of injury associated with the increased load, pointing out complex adaptation
65 strategies of the upper limb.

66 **METHODS**

67 *Data collection*

68 The raw data previously used by Martinez et al. (2020) was used. Forty participants who had
69 no history of upper limb diseases performed a box handling task. The research protocol was
70 approved by the University of Montréal ethics committee (n° 15-016-CERES-P). All
71 participants provided their informed consent prior to the experimentation. A brief presentation
72 of the experimental setup is described hereafter, see supplementary material for a detailed
73 description.

74 The kinematics of the participants' trunk and right upper limb, and that of the box were
75 tracked using 42 reflective markers. Bipolar surface EMG electrodes were used to measure
76 the activation of 10 muscles: anterior, median and posterior deltoids, biceps, triceps,
77 pectoralis major, latissimus dorsi, upper and lower trapezius and serratus anterior.
78 Infraspinatus, supraspinatus and subscapularis activations were recorded using indwelling
79 electrodes. The linear envelopes of the EMG signals were normalized to the maximal
80 voluntary contraction (Dal Maso et al., 2016). The participants moved a box (6 or 12 kg)
81 between two shelves from hip to eye level. Forces and moments between the right hand and
82 the box were measured using a six-dimensional force sensor.

83 *Neuro-musculoskeletal model*

84 A musculoskeletal model was developed in Opensim (Delp et al., 2007) from the shoulder
85 model of Wu (2016). The acromioclavicular and glenohumeral joints were both modelled as
86 3-DOF joints, while the sternoclavicular joint, the elbow and wrist were each modelled as 2-
87 DOF joint. The glenohumeral joint DOFs sequence was plane of elevation, elevation and axial
88 rotation (Wu et al., 2005). The generic model was first anthropometrically scaled to match the
89 markers positions during a static trial in the anatomical position. The joint angles and
90 moments were predicted using Opensim's inverse kinematics and inverse dynamics,
91 respectively (Delp et al., 2007). Our study was focused on the glenohumeral joint DOFs and
92 the muscles acting on it. Out of the 17 musculotendon units actuating the glenohumeral joint,
93 three had no experimental EMG. The scaled models were further personalized by calibrating
94 their neuromuscular parameters (e.g. optimal fiber length) using the CEINMS toolbox
95 (Pizzolato et al., 2015). The personalized models were then used to predict muscle forces and
96 fiber contraction velocities in CEINMS using an EMG-assisted scheme, while implementing a
97 fiber-tendon equilibrium constraint. The calibration and muscle force prediction processes are
98 described in supplementary material.

100 We calculated the glenohumeral joint 3-DOF powers as the product of their respective
101 generalized moments and angular velocities. The muscle fiber power was calculated as the
102 product of the fiber's tension and its contractile velocity. DOF and fiber powers were reported
103 for men and women with both loads. To evaluate the function of each DOF and each fiber
104 during the box-handling tasks, we calculated four indices that describe the mechanical
105 behavior of an entity as a strut, a spring, a motor and a damper (i.e., function indices). The
106 indices were defined to have a cumulative sum of 100% and are fully described in Lai (2019)
107 and Qiao and Jindrich (2016). Further details about these indices can be found in
108 supplementary material. Briefly, an entity that has a dominant strut behavior would generate
109 large forces with little fluctuation in its length or angle. A spring-like behavior manifests itself
110 with energy storage or release often synchronized with the compression and extension phases
111 of the movement. Since the task of interest involved mainly a thoraco-humeral elevation, we
112 defined the compression phase as the phase beginning with the lifting of the box from the
113 shelf to the moment when the box is the closest to the participant, while the rest of the trial is
114 the extension phase. An entity, acting like a motor, would generate mainly positive work
115 throughout the task. Finally, a damper-like behavior would stand for a dominant negative
116 work generation. To obtain dimensionless indices for muscle fibers, the strut index was
117 normalized with respect to the fiber's optimal length obtained with the model calibration.

118 The effects of sex and load on the glenohumeral DOF and muscle fibers powers, as well as
119 their function indices were evaluated using a two-way nonparametric ANOVA with repeated
120 measures on the load (Pataky et al., 2015). Statistical significance was fixed at 0.05. For the
121 1D analysis, the family-wise error for all clusters was respected using a Bonferroni correction
122 to account for the number of DOFs and muscle. On the other hand, the p-values reported for

123 the function indices (OD analysis) are the ones obtained from a Holm-Bonferroni correction,
124 to maintain the power of the analysis, despite running the tests for four indices.

125 **RESULTS**

126 The sex had no significant effect on the joint power, while the load had a significant effect on
127 the power of the glenohumeral elevation ($p < 0.05$; Fig. 1). The glenohumeral plane of
128 elevation and axial rotation had power peaks higher than those calculated for the elevation.
129 These peaks occurred close to the transition from the compression to the extension phase (Fig.
130 1). The net joint power was mainly the result of the anterior deltoid, biceps and latissimus
131 dorsi fiber powers, followed by the infraspinatus and supraspinatus, two rotator cuff muscles
132 (Fig. 2). No major effects of sex, load, nor their interaction were observed on the fibers
133 power.

134 All glenohumeral DOF had a minimal strut-like behavior with no significant effect of sex or
135 load ($p > 0.05$; Fig. 3). The spring-like behavior was not a main function for any of the DOF;
136 however, it was usually more present in the glenohumeral axial rotation, irrespective of the
137 load or sex ($p > 0.05$). The load affected the elevation damper ($p = 0.012$) and motor ($p = 0.035$)
138 behaviors. Both men and women relied on their glenohumeral plane of elevation and
139 elevation as prime motors. For the 6 kg lifting task, women relied more on their plane of
140 elevation to drive the motion with a motor index of $66 \pm 15\%$, whereas men preferred their
141 glenohumeral elevation ($68 \pm 23\%$). For the 12 kg task, women did not change their power
142 strategy (glenohumeral plane motor index: $60 \pm 16\%$), while men moved the box by using
143 both their plane of elevation ($48 \pm 20\%$) and elevation ($46 \pm 28\%$) as motors. The damping
144 action was ensured by the glenohumeral axial rotation for women and men during the 6 kg
145 trial. However, as the load increased, so did the damping action of the two other DOFs.

146 Most muscles had a mainly strut-like behavior, with rotator cuff muscles showcasing the
147 highest values (on average 90%). The biceps had, almost, no strut-like but a spring-like
148 behavior irrespective of the trial, followed by the posterior deltoid (Fig. 4). Following the
149 strut-like behavior, the muscles had either a damper or a motor-like tendencies, except for the
150 bicep's fibers. The clavicular head of the pectoralis major had a motor-like behavior for all
151 trials. The load also had an effect on the damping behavior of the latissimus dorsi and
152 subscapularis ($p < 0.015$), on the spring behavior of the posterior deltoid and the infraspinatus
153 ($p < 0.015$) and the strut behavior of the posterior deltoid, subscapularis and biceps ($p < 0.015$).
154 An effect of the interaction sex-load was only observed on the biceps strut behavior
155 ($p < 0.015$).

156 **DISCUSSION**

157 We implemented an analysis of the glenohumeral joint DOF and its muscle fibers based on
158 their mechanical energy to improve our understanding of the glenohumeral joint functions
159 during a lifting task. The predicted behavioral indices provided evidence supporting our
160 hypotheses regarding glenohumeral DOF and muscle functions. The limited strut indices of
161 the glenohumeral joint highlighted its large range of motion, whereas the large strut behavior
162 of muscle fibers, particularly the rotator cuff, emphasized their stabilizing function. Finally,
163 the predicted indices highlighted the sensitivity of kinematic and activation strategies to load
164 and sex.

165 *Glenohumeral joint: a design for a wide range of motion*

166 The complexity of the glenohumeral joint morphology has evolved to ensure a large range of
167 motion (Larson, 2009). With thoracohumeral elevation, the scapula is reoriented to maintain
168 congruency with the humeral head, and the humerus is externally rotated to avoid
169 impingement (Ludewig et al., 2009; Stokdijk et al., 2003). The effect of the scapula

170 orientation can be observed in the power evolution of the glenohumeral DOFs. While the task
171 involved mainly a change in potential energy of the box (thoracohumeral elevation)
172 (supplementary data, Fig. S2), the power of the glenohumeral elevation was smaller than the
173 other DOFs. Additionally, the occurrence of power peaks close to the transition between
174 pulling and pushing the box pointed out a strategy where participants relied on a sudden
175 increase in the box momentum to drive its elevation, confirmed by the change in box vertical
176 velocity. Women, who exhibit less upper body strength than men (Janssen et al., 2000), had a
177 steeper increase of the box vertical velocity at this transition (supplementary data, Fig. S3).
178 This could potentially explain the increased risk of injury for women, as the upper-arm
179 velocity was correlated with shoulder complaints (Balogh et al., 2019).

180 The design of the glenohumeral joint to cater to both mobility and stability can be observed in
181 its DOF strut coefficients. The box handling task did not reach extreme upper limb positions
182 yet was highly demanding of the shoulder. However, the strut index remained relatively low,
183 suggesting that the glenohumeral joint has a high compliancy, which would facilitate the
184 upper limb motor control and movement regulation. This is coherent with the glenohumeral
185 joint architecture that is optimal for large and precise displacements (Arias-Martorell, 2019).
186 This optimization impacted strongly the orientation of the scapula, which has been linked to
187 the throwing function of the upper limb, and enabled the use of elastic energy stored during
188 external rotation to increase the power generated for high-speed throwing (Roach et al.,
189 2013). This could possibly explain the high spring index observed for the humeral axial
190 rotation. Besides its spring function, the axial rotation behaved mainly as a damper, which
191 could point out functions of the passive structures (shoulder capsule and ligaments) that
192 would behave mostly as elastic components, stiffening with the glenohumeral axial rotation
193 (Burkart and Debski, 2002; Wilk et al., 1997). As the load increased, this passive damping
194 was probably no longer enough, thus the increase in the other DOFs input to the damping, and

195 possibly glenohumeral stability, at the expense of the elevation's motor behavior, and the box
196 vertical velocity.

197 *Adaptations to load within the joint*

198 The main motor behavior was ensured by the glenohumeral elevation and plane of elevation.
199 Women opted to use their glenohumeral plane of elevation to drive the movement. While their
200 strategy did not change between loads, men adapted theirs as the load increased, distributing
201 the motor load more equally between the actuators of the glenohumeral elevation and plane of
202 elevation. Participants have been reported to increase the use of their lower limbs with load
203 increase, with men relying on their hip vertical displacement more than women (Martinez et
204 al., 2020). The 12 kg task might have been taxing for both men and women's glenohumeral
205 joint. For men, however, relying on their lower limb, they decreased the motor demand on the
206 glenohumeral elevation, favoring stability. Women, on the other hand, might have already
207 strained their shoulder for the 6 kg task, which led them to seek assistance from their elbow
208 for the 12 kg one (Martinez et al., 2019). This observed adaptation could possibly shed a light
209 on neural control schemes that could start within the same structure (glenohumeral), before
210 seeking neighboring ones (distal joints). This points out the importance of the coupling of a
211 local and global kinematic analysis to gain a deeper understanding of the human motion.

212 *Fiber power adaptation to load*

213 Unlike joint power, the fiber powers did not have any significant increase with the load,
214 despite the significant muscle activation increase shown in Bouffard et al. (2019). This power
215 invariance pointed out a possible decrease in the fiber contraction velocity as the load
216 increased. This could be a direct effect of the decrease of the glenohumeral range of motion
217 with the load (Martinez et al., 2019). This decrease could also be linked to the change in
218 compliance of the muscle-tendon unit. As the load increased from 6 to 12 kg, the stiffness of
219 the tendon might have increased (Raiteri et al., 2018), impacting the fiber compliance, which

220 is reported to affect its power generation and efficiency (Fenwick et al., 2017). This potential
221 adaptation strategy would decrease injury risk at higher loads. As women have more
222 compliant tendons compared to men (Kubo et al., 2003), this could account in part for
223 women's higher injury rate, particularly as they rely more on speed to drive the box.

224 *Fiber function between actuation and stability*

225 The highest strut like behavior in muscles was showcased by the infraspinatus and
226 subscapularis. This was consistent with their architecture, having relatively short fibers and
227 large physiological cross-sectional areas, which enables them to generate large forces over a
228 short range of deformation (Gobbi, 2017). Overall, most of the muscles displayed a strut-like
229 behavior for the studied task, which implies a high fiber force with a minimal length change,
230 which supports our initial hypothesis. Unlike most upper limb muscles, the biceps had a main
231 spring-like behavior, storing and releasing energy. This behavior is consistent with its
232 architecture, as slender muscles with long tendons are reported to be favorably designed for
233 energy saving (Biewener, 2009). However, mechanical energy storage remains costly from a
234 chemical energy perspective.

235 The muscle ability to quickly actuate a joint depends on the speed and the type of contraction.
236 A muscle would more efficiently generate a higher torque during concentric activations at
237 higher speeds (Tillin et al., 2018). This might explain the significant decrease in the motor
238 function of the clavicular head of the pectoralis major as the load increased, since the
239 contraction velocity decreased, limiting the fiber force potential. This could also explain why
240 women chose to approach the box to their trunk, as it gave them higher potential for a
241 concentric explosive contraction. However, an explosive contraction without sufficient
242 muscle strength and control, particularly for higher loads, might increase injury risk (Davies
243 and Matheson, 2001). This might explain why the damper behavior of some muscles
244 increased with the load, as this function should help in the stabilization of the humeral head.

245 The effect of the load on the strut, spring and damper behavior further points to the
246 complexity of the glenohumeral joint stabilization, as it involves more than just the rotator
247 cuff muscles (Lee and An, 2002; Yanagawa et al., 2008).

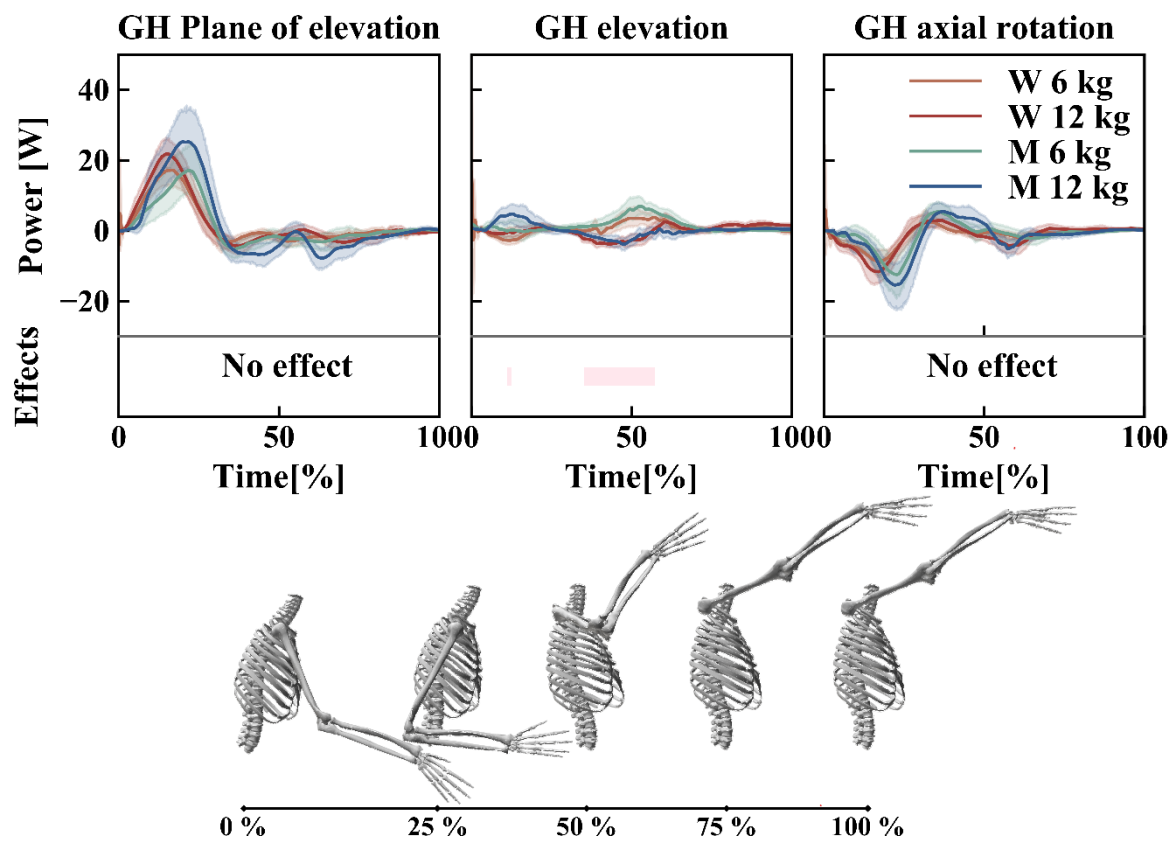
248 *Energetic approaches to complement the upper limb understanding*

249 The musculoskeletal structure is a transducer that converts chemical energy into mechanical
250 work (Wilkie, 1975). Accordingly, energetic approaches could potentially offer a
251 complementary and insightful understanding to the classical biomechanical analysis of forces
252 and kinematics (Guo et al., 2003; Siegel et al., 2004). Similarly, within our study, we could
253 gain insight into the intricate functions of the different glenohumeral joint DOF, without the
254 need to analyze unidirectional movements (Hawkes et al., 2019). The use of the four function
255 indices enabled a fair analysis of the different muscles within their physiological abilities.
256 Indeed, while the infraspinatus and subscapularis had low power magnitude, their role in
257 glenohumeral stability was emphasized by their strut index. This reinforces our understanding
258 of the stabilizing potential of the rotator cuff muscles, particularly as their characteristics are
259 still not well understood (Sangwan et al., 2015). These indices could also be used in the
260 development of ergonomic work strategies that go beyond the joint repartition (Martinez et
261 al., 2020) of the task.

262 Our study had some limitations. We chose to normalize the shelves height to the participants
263 to reduce bias against women. For an energetic approach, this led to differences in the
264 potential energy of the box. However, it was expected that the gender-related differences
265 would only be exacerbated in a working environment. The use of an energetic approach is
266 also limited by the power magnitude sensitivity to the scapula kinematic errors, particularly
267 those related to the soft tissue artefact (Blache et al., 2016). As for the indices' definition, the
268 main limitation relied in the need of a compression and extension phases within the studied
269 trial. While this could be relatively easy to define for cyclic tasks: such as handcycling, it is

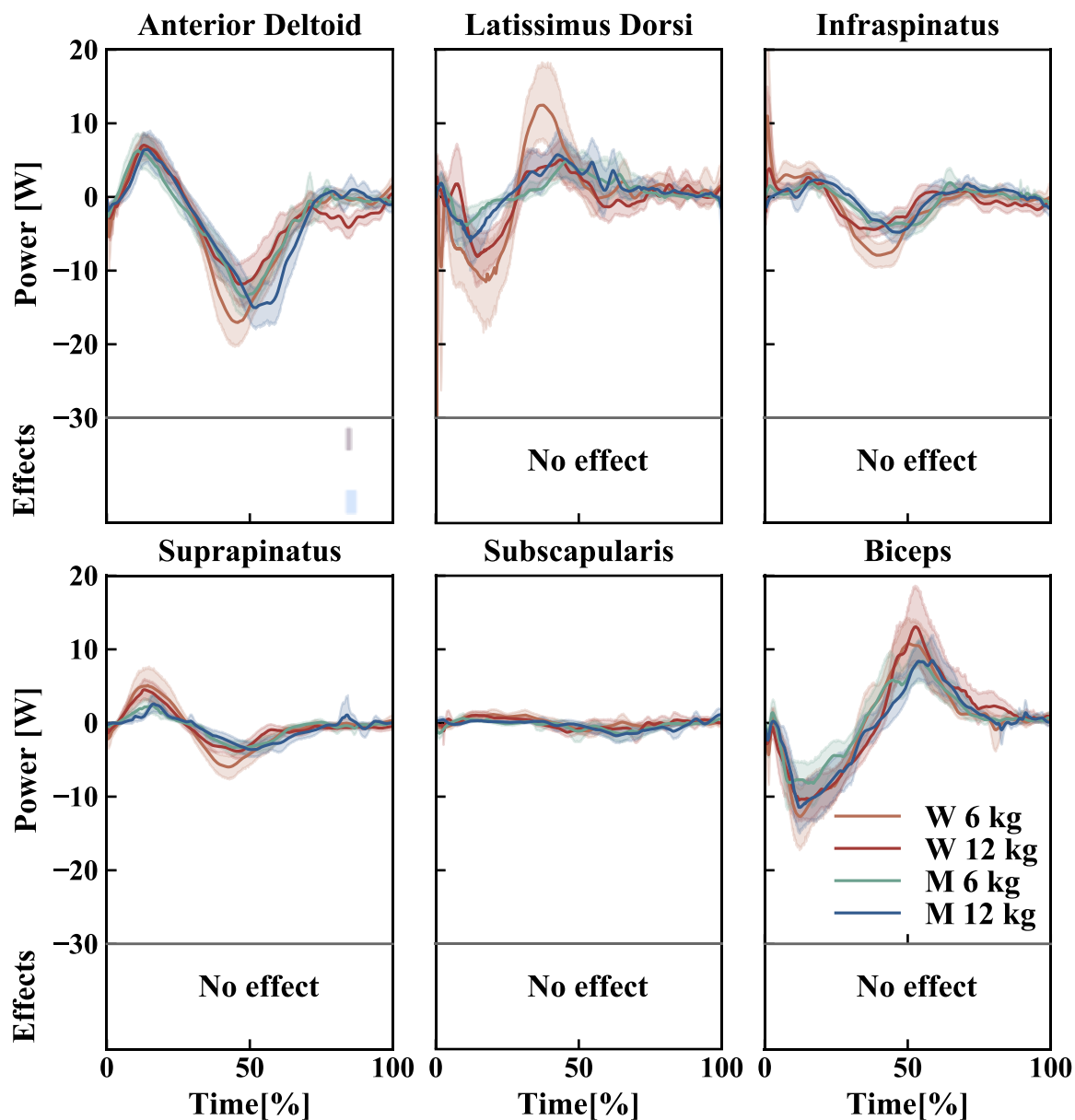
270 less straightforward for the majority of the upper limb tasks. Finally, the strut index is defined
271 relatively to a given length that could change the overall distribution of the muscle functions.
272 Unlike in Lai et al. (2019), there is no specific known behavior of the upper limb tendons or
273 muscles. Accordingly, we decided to use the fiber optimal length to make the strut index
274 dimensionless. This choice should circumvent introducing any task, participant or muscle
275 induced bias to the study. In the future, more research needs to be done to find an optimal
276 parameter for normalizing the upper limb strut index.

277 The implemented index-based approach enabled a more comprehensive understanding of the
278 upper limb motor control strategies during a box handling task and a summarized insight in the
279 function of the various muscles. The indices highlighted particularities of the glenohumeral
280 joint (large range of motion) and its muscles (stabilizing function), as well as sex-dependent
281 adaptation strategies to load, supporting our initial hypotheses. This approach might improve
282 our understanding of the upper limb by offering additional insight into its motor control
283 strategies, its components functional alterations related to pathologies or its adaptations to
284 external parameters.

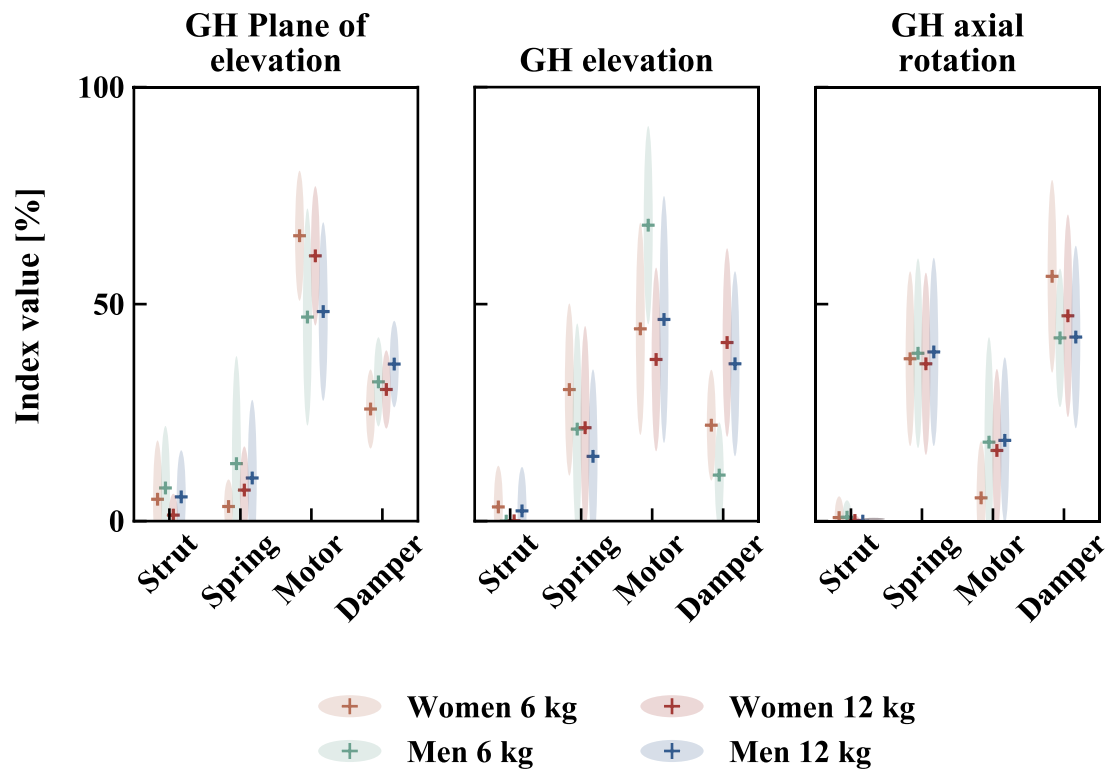


286

287 *Fig. 1. Glenohumeral joint power generated by women (W) and men (M) during the box (6 or*
 288 *12 kg) lifting tasks: solid line: mean value, hue: 95% confidence interval. In the bottom part of*
 289 *the graphs, pink bands correspond to the load effect.*



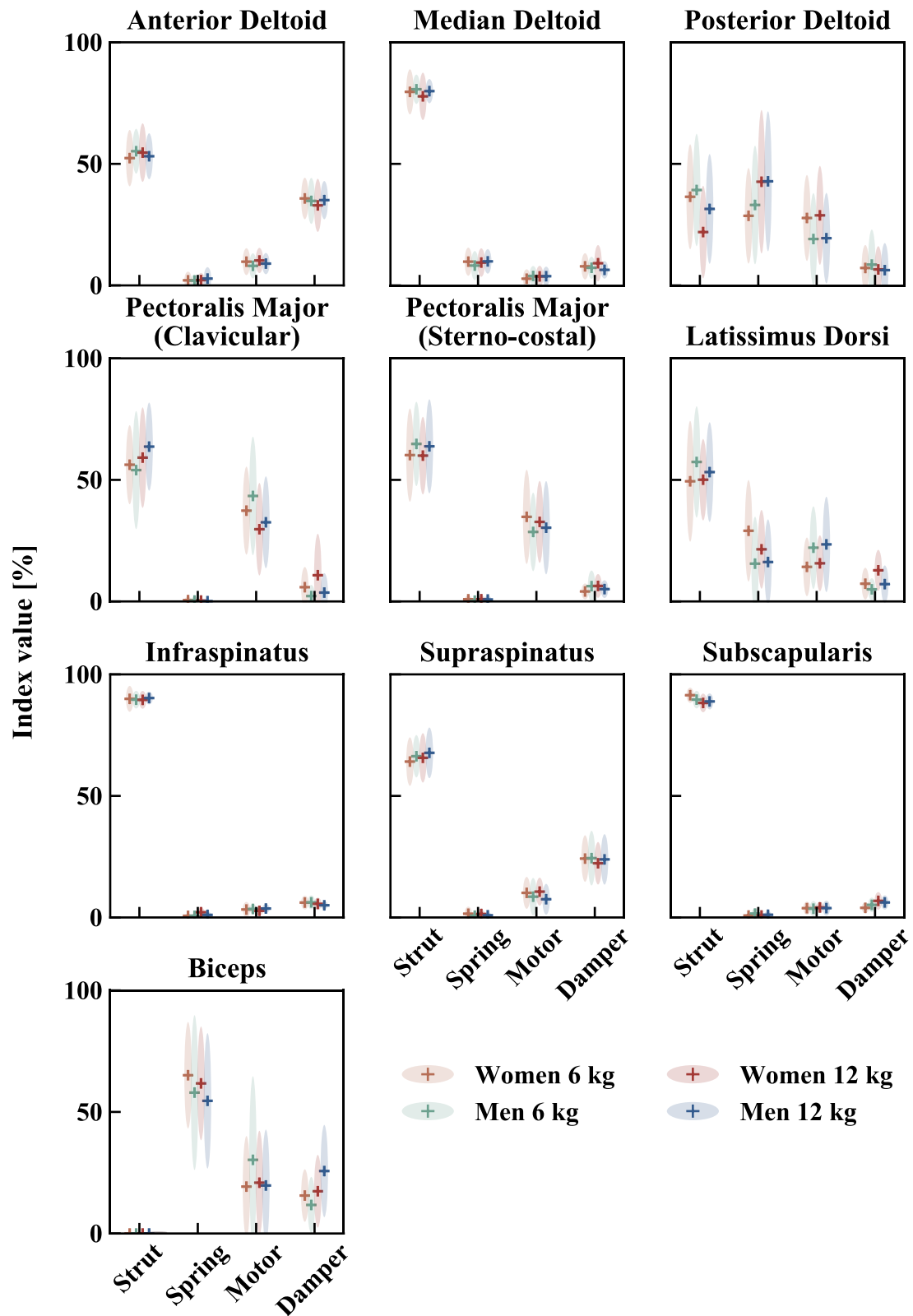
291
 292 *Fig. 2. Power generated by muscle fibres during the box (6 and 12 kg) lifting tasks for women*
 293 *(W) and men (M); solid line: mean value, hue: 95% confidence interval, blue bands: sex effect,*
 294 *purple bands: sex-load effect.*



296

297 *Fig. 3. Mean values of the four joint indices with a load of 6 and 12 kg for women and men.*

298



299

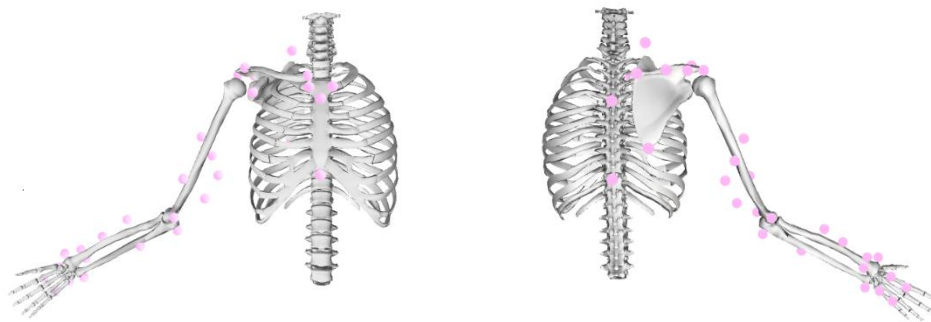
300 *Fig. 4. Mean values of the four muscle fiber indices with a load of 6 or 12 kg for women and*

301 *men.*

302 **SUPPLEMENTARY MATERIAL**

303 *Data collection*

304 Forty participants (20 women; 23.12 ± 3.1 years; 173.5 ± 9.5 cm; 68.1 ± 12.7) took part in this
305 study. They did not suffer from any significant disability related to their upper limbs or backs.
306 The participants first performed a static trial to anthropometrically scale the musculoskeletal
307 model. Then, they moved a box from a shelf at hip level to a shelf at eye level. The shelves
308 heights were adjusted to the height of each participant. The participants performed three lifts
309 for each mass (6 and 12 kg). The order of the lifts was randomized. A 30 s rest period
310 between lifts was given for recovery with increased time if needed. Assuming symmetry
311 between the right and left side during this task, only the right side was analyzed. A 6-degree-
312 of-freedom force sensor (Sensix, Poitiers, France) was mounted on the right handle of the box
313 to measure the contact forces between the box and the participant's hand. A threshold of 5 N
314 was used to detect the start and end of each trial. Following the recommendations of Jackson
315 et al. (2012), 34 reflective markers were used to track the trunk and upper limb kinematics
316 (Fig. S1). Eight markers positions on the box corners were used to track the box kinematics.



317

318 *Fig. S1. The position of the markers used to track the trunk and upper limb kinematics.*

319 *Neuro-musculoskeletal model*

320 To personalize the neuro-musculoskeletal model, the various parameters involved in the
321 activation and contraction dynamics were calibrated using experimental EMG. One trial per
322 participant lifting a 6 kg load was used for calibration. The calibration aimed to find musculo-

323 tendon parameters that simultaneously minimized the inverse dynamic torques tracking
 324 quadratic error and the ratio of the glenohumeral joint shear to compressive contact forces,
 325 while driving the model using the experimental EMG. A penalty was used to avoid normalized
 326 fiber length outside the physiological range throughout the calibration trial. This objective
 327 function enabled the respect of the glenohumeral joint non-dislocation constraint without the
 328 need to explicitly include it in the muscle force prediction algorithm.

329 The calibrated models were then used to predict muscle forces through an EMG-informed
 330 algorithm. The optimization scheme adjusted the available experimental EMG envelopes and
 331 synthesized the excitations that were not measured experimentally. The adjusted and
 332 synthesized excitations minimized three terms: 1- inverse dynamics joint moments tracking
 333 error, 2- experimental envelopes tracking error, 3- the sum of squared excitations for all lines
 334 of actions. The weights used for the various terms were chosen to achieve a good balance
 335 between joint moments and excitations tracking (Sartori et al., 2014).

336 *Function indices*

337 The function indices calculation was based on the formulae presented in (Lai et al., 2019; Qiao
 338 and Jindrich, 2016). The strut index is the ratio of the mechanical work generated by the entity
 339 during the box lifting task to the sum of the force norm generated. Accordingly, the index can
 340 be defined as follows:

$$341 \quad I_{strut,DOF} = \max \left(1 - \frac{(t_{end} - t_{beg}) \int_{t_{start}}^{t_{end}} |P_{DOF}| dt}{\int_{t_{start}}^{t_{end}} |M_{DOF}| dt}, 0 \right) \times 100\%$$

$$342 \quad I_{strut,muscle} = \max \left(1 - \frac{(t_{end} - t_{beg}) \int_{t_{start}}^{t_{end}} |P_{muscle}| dt}{l_{opt} \int_{t_{start}}^{t_{end}} |F_{muscle}| dt}, 0 \right) \times 100\%$$

343 with P_{DOF} and P_{muscle} the mechanical powers of the DOF and the fiber, respectively; M_{DOF} the
 344 DOF moment and F_{muscle} the fiber force. The optimal length of the fiber (l_{opt}) was used to
 345 obtain a dimensionless index. The lifting task started at t_{beg} and finished at t_{end} .

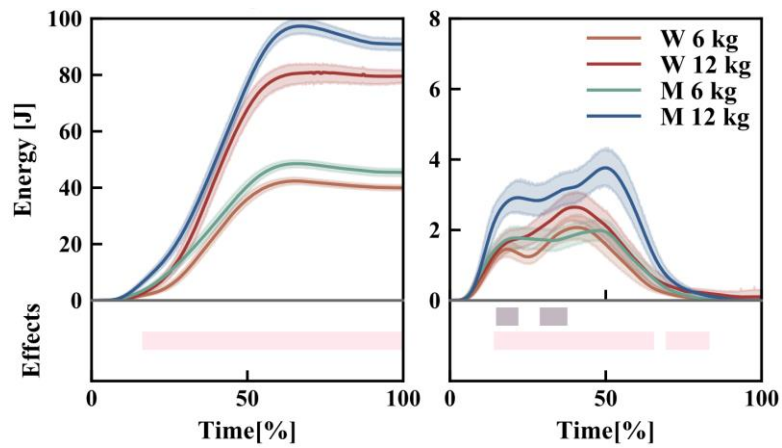
346 The other indices were calculated similarly for both the glenohumeral DOFs and muscles. They
 347 were calculated as follows:

$$348 \quad I_{spring} = \frac{2 \cdot \min(|W_{com}^-|, |W_{ext}^+|)}{|W_{tot}^+| + |W_{tot}^-|} \times (100\% - I_{strut})$$

$$349 \quad I_{motor} = \frac{|W_{tot}^+| - \min(|W_{com}^-|, |W_{ext}^+|)}{|W_{tot}^+| + |W_{tot}^-|} \times (100\% - I_{strut})$$

$$350 \quad I_{damper} = \frac{|W_{tot}^-| - \min(|W_{com}^-|, |W_{ext}^+|)}{|W_{tot}^+| + |W_{tot}^-|} \times (100\% - I_{strut})$$

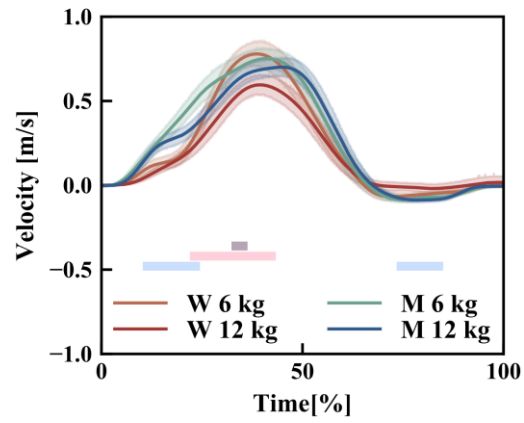
351 where $|W_{tot}^+|, |W_{tot}^-|$ were respectively the total positive and negative works generated by the
 352 entity. $|W_{com}^-|$ and $|W_{ext}^+|$ were respectively the negative work during the compression phase
 353 and the positive work during the extension phase.



354

355 *Fig. S2. Left: potential energy of the box with reference at hip level solid line, right: Kinetic*
 356 *energy of the box with the box state at t=0 as reference value: mean value, hue: 95% confidence*
 357 *interval, pink bands: load effect, purple bands: sex-load effect.*

358 *Note: The difference in potential energy between men and women was due to the height of the*
 359 *shelves that has been normalized to participants height (women: 167.7 ± 7.1 cm, men: 179.3 ± 7.9*
 360 *cm).*



361

362 *Fig. S3. Vertical velocity of the box (6 or 12 kg) for women (W) and men (M): solid line: mean value,*

363 *hue: 95% confidence interval, blue bands: sex effect, pink bands: load effect, purple bands: sex-load*

364 *effect.*

365 **ACKNOWLEDGMENT**

366 This research was undertaken thanks, in part to funding from the Canada First Research Excellence
367 Fund through the TransMedTech Institute. We acknowledge the support of the Natural Sciences and
368 Engineering Research Council of Canada (NSERC), [RGPIN-2019-04978]. This study was carried out
369 within the framework of the Associated International Laboratory EVASYM.

370 **CONFLICT OF INTEREST**

371 The authors do not have any conflict of interest that could inappropriately influence this manuscript.

- 372 Arias-Martorell, J., 2019. The morphology and evolutionary history of the glenohumeral joint
373 of hominoids: A review. *Ecology and Evolution* 9, 703–722.
374 <https://doi.org/10.1002/ece3.4392>
- 375 Balogh, I., Arvidsson, I., Björk, J., Hansson, G.-Å., Ohlsson, K., Skerfving, S., Nordander, C.,
376 2019. Work-related neck and upper limb disorders – quantitative exposure–response
377 relationships adjusted for personal characteristics and psychosocial conditions. *BMC*
378 *Musculoskeletal Disorders* 20, 139. <https://doi.org/10.1186/s12891-019-2491-6>
- 379 Biewener, A.A., 2016. Locomotion as an emergent property of muscle contractile dynamics. *J*
380 *Exp Biol* 219, 285–294. <https://doi.org/10.1242/jeb.123935>
- 381 Biewener, A.A., 2009. Muscle and Tendon Energy Storage, in: Binder, M.D., Hirokawa, N.,
382 Windhorst, U. (Eds.), *Encyclopedia of Neuroscience*. Springer, Berlin, Heidelberg, pp.
383 2492–2496. https://doi.org/10.1007/978-3-540-29678-2_3657
- 384 Blache, Y., Dumas, R., Lundberg, A., Begon, M., 2016. Main component of soft tissue artifact
385 of the upper-limbs with respect to different functional, daily life and sports movements.
386 *J. Biomech.* <https://doi.org/10.1016/j.jbiomech.2016.10.019>
- 387 Bouffard, J., Martinez, R., Plamondon, A., Côté, J.N., Begon, M., 2019. Sex differences in
388 glenohumeral muscle activation and coactivation during a box lifting task. *Ergonomics*
389 1–12. <https://doi.org/10.1080/00140139.2019.1640396>
- 390 Burkart, A.C., Debski, R.E., 2002. Anatomy and Function of the Glenohumeral Ligaments in
391 Anterior Shoulder Instability. *Clinical Orthopaedics and Related Research*® 400, 32.
- 392 Dal Maso, F., Marion, P., Begon, M., 2016. Optimal Combinations of Isometric Normalization
393 Tests for the Production of Maximum Voluntary Activation of the Shoulder Muscles.
394 *Arch. Phys. Med. Rehabil.* 97, 1542-1551.e2.
395 <https://doi.org/10.1016/j.apmr.2015.12.024>
- 396 Davies, G.J., Matheson, J.W., 2001. Shoulder Plyometrics. *Sports Medicine and Arthroscopy*
397 *Review* 9, 1–18.
- 398 Delp, S.L., Anderson, F.C., Arnold, A.S., Loan, P., Habib, A., John, C.T., Guendelman, E.,
399 Thelen, D.G., 2007. OpenSim: Open-Source Software to Create and Analyze Dynamic
400 Simulations of Movement. *IEEE Trans. Biomed. Eng.* 54, 1940–1950.
401 <https://doi.org/10.1109/TBME.2007.901024>
- 402 Dickinson, M.H., Farley, C.T., Full, R.J., Koehl, M. a. R., Kram, R., Lehman, S., 2000. How
403 Animals Move: An Integrative View. *Science* 288, 100–106.
404 <https://doi.org/10.1126/science.288.5463.100>

405 Fenwick, A.J., Wood, A.M., Tanner, B.C.W., 2017. Effects of cross-bridge compliance on the
406 force-velocity relationship and muscle power output. *PLoS One* 12.
407 <https://doi.org/10.1371/journal.pone.0190335>

408 Gobbi, A., 2017. *Bio-orthopaedics: a new approach*. Springer Berlin Heidelberg, New York,
409 NY.

410 Guo, L.-Y., Su, F.-C., Wu, H.-W., An, K.-N., 2003. Mechanical energy and power flow of the
411 upper extremity in manual wheelchair propulsion. *Clin Biomech* 18, 106–114.
412 [https://doi.org/10.1016/S0268-0033\(02\)00177-8](https://doi.org/10.1016/S0268-0033(02)00177-8)

413 Hawkes, D.H., Khaiyat, O.A., Howard, A.J., Kemp, G.J., Frostick, S.P., 2019. Patterns of
414 muscle coordination during dynamic glenohumeral joint elevation: An EMG study.
415 *PLoS ONE* 14, e0211800. <https://doi.org/10.1371/journal.pone.0211800>

416 Inman, V.T., Saunders, J.B. dec M., Abbott, L.C., 1996. Observations of the Function of the
417 Shoulder Joint. *Clinical Orthopaedics and Related Research* 330, 3.

418 Jackson, M., Michaud, B., Tétreault, P., Begon, M., 2012. Improvements in measuring shoulder
419 joint kinematics. *J. Biomech.* 45, 2180–2183.
420 <https://doi.org/10.1016/j.jbiomech.2012.05.042>

421 Janssen, I., Heymsfield, S.B., Wang, Z., Ross, R., 2000. Skeletal muscle mass and distribution
422 in 468 men and women aged 18–88 yr. *Journal of Applied Physiology* 89, 81–88.
423 <https://doi.org/10.1152/jappl.2000.89.1.81>

424 Kubo, K., Kanehisa, H., Fukunaga, T., 2003. Gender differences in the viscoelastic properties
425 of tendon structures. *Eur J Appl Physiol* 88, 520–526. <https://doi.org/10.1007/s00421-002-0744-8>

427 Lai, A.K.M., Biewener, A.A., Makeling, J.M., 2019. Muscle-specific indices to characterise the
428 functional behaviour of human lower-limb muscles during locomotion. *J. Biomech.* 89,
429 134–38. <https://doi.org/10.1016/j.jbiomech.2019.04.027>

430 Lappin, A.K., Monroy, J.A., Pilarski, J.Q., Zepnewski, E.D., Pierotti, D.J., Nishikawa, K.C.,
431 2006. Storage and recovery of elastic potential energy powers ballistic prey capture in
432 toads. *Journal of Experimental Biology* 209, 2535–2553.
433 <https://doi.org/10.1242/jeb.02276>

434 Larson, S.G., 2009. Evolution of the Hominin Shoulder: Early Homo, in: Grine, F.E., Fleagle,
435 J.G., Leakey, R.E. (Eds.), *The First Humans – Origin and Early Evolution of the Genus*
436 *Homo*. Springer Netherlands, Dordrecht, pp. 65–75. https://doi.org/10.1007/978-1-4020-9980-9_7

438 Lee, S.-B., An, K.-N., 2002. Dynamic Glenohumeral Stability Provided by Three Heads of the
439 Deltoid Muscle. *Clinical Orthopaedics and Related Research* 400, 40.

440 Ludewig, P.M., Phadke, V., Braman, J.P., Hassett, D.R., Cieminski, C.J., LaPrade, R.F., 2009.
441 Motion of the Shoulder Complex During Multiplanar Humeral Elevation. *J Bone Joint*
442 *Surg Am* 91, 378–389. <https://doi.org/10.2106/JBJS.G.01483>

443 Martinez, R., Assila, N., Goubault, E., Begon, M., 2020. Sex differences in upper limb
444 musculoskeletal biomechanics during a lifting task. *Applied Ergonomics* 86, 103106.
445 <https://doi.org/10.1016/j.apergo.2020.103106>

446 Martinez, R., Bouffard, J., Michaud, B., Plamondon, A., Côté, J.N., Begon, M., 2019. Sex
447 differences in upper limb 3D joint contributions during a lifting task. *Ergonomics* 62,
448 682–693. <https://doi.org/10.1080/00140139.2019.1571245>

449 Pataky, T.C., Vanrenterghem, J., Robinson, M.A., 2015. Zero- vs. one-dimensional, parametric
450 vs. non-parametric, and confidence interval vs. hypothesis testing procedures in one-
451 dimensional biomechanical trajectory analysis. *Journal of Biomechanics* 48, 1277–
452 1285. <https://doi.org/10.1016/j.jbiomech.2015.02.051>

453 Pizzolato, C., Lloyd, D.G., Sartori, M., Ceseracciu, E., Besier, T.F., Fregly, B.J., Reggiani, M.,
454 2015. CEINMS: A toolbox to investigate the influence of different neural control

455 solutions on the prediction of muscle excitation and joint moments during dynamic
456 motor tasks. *J. Biomech.* 48, 3929–3936.
457 <https://doi.org/10.1016/j.jbiomech.2015.09.021>

458 Qiao, M., Jindrich, D.L., 2016. Leg joint function during walking acceleration and deceleration.
459 *Journal of Biomechanics* 49, 66–72. <https://doi.org/10.1016/j.jbiomech.2015.11.022>

460 Raiteri, B.J., Cresswell, A.G., Lichtwark, G.A., 2018. Muscle-tendon length and force affect
461 human tibialis anterior central aponeurosis stiffness in vivo. *PNAS* 115, E3097–E3105.
462 <https://doi.org/10.1073/pnas.1712697115>

463 Richardson, A.G., Slotine, J.-J.E., Bizzi, E., Tresch, M.C., 2005. Intrinsic Musculoskeletal
464 Properties Stabilize Wiping Movements in the Spinalized Frog. *J. Neurosci.* 25, 3181–
465 3191. <https://doi.org/10.1523/JNEUROSCI.4945-04.2005>

466 Roach, N.T., Venkadesan, M., Rainbow, M.J., Lieberman, D.E., 2013. Elastic energy storage
467 in the shoulder and the evolution of high-speed throwing in Homo. *Nature* 498, 483–
468 486. <https://doi.org/10.1038/nature12267>

469 Sangwan, S., Green, R.A., Taylor, N.F., 2015. Stabilizing characteristics of rotator cuff
470 muscles: a systematic review. *Disability and Rehabilitation* 37, 1033–1043.
471 <https://doi.org/10.3109/09638288.2014.949357>

472 Sartori, M., Farina, D., Lloyd, D.G., 2014. Hybrid neuromusculoskeletal modeling to best track
473 joint moments using a balance between muscle excitations derived from
474 electromyograms and optimization. *J. Biomech.* 47, 3613–3621.
475 <https://doi.org/10.1016/j.jbiomech.2014.10.009>

476 Siegel, K.L., Kepple, T.M., Stanhope, S.J., 2004. Joint moment control of mechanical energy
477 flow during normal gait. *Gait & Posture* 19, 69–75. [https://doi.org/10.1016/S0966-
478 6362\(03\)00010-9](https://doi.org/10.1016/S0966-6362(03)00010-9)

479 Stokdijk, M., Eilers, P.H.C., Nagels, J., Rozing, P.M., 2003. External rotation in the
480 glenohumeral joint during elevation of the arm. *Clinical Biomechanics* 18, 296–302.
481 [https://doi.org/10.1016/S0268-0033\(03\)00017-2](https://doi.org/10.1016/S0268-0033(03)00017-2)

482 Tillin, N.A., Pain, M.T.G., Folland, J.P., 2018. Contraction speed and type influences rapid
483 utilisation of available muscle force: neural and contractile mechanisms. *J Exp Biol* 221,
484 *jeb193367*. <https://doi.org/10.1242/jeb.193367>

485 Veeger, H.E.J., van der Helm, F.C.T., 2007. Shoulder function: The perfect compromise
486 between mobility and stability. *J. Biomech* 40, 2119–2129.
487 <https://doi.org/10.1016/j.jbiomech.2006.10.016>

488 Wilk, K.E., Arrigo, C.A., Andrews, J.R., 1997. Current Concepts: The Stabilizing Structures of
489 the Glenohumeral Joint. *J Orthop Sports Phys Ther* 25, 364–379.
490 <https://doi.org/10.2519/jospt.1997.25.6.364>

491 Wilkie, D.R., 1975. Muscle as a thermodynamic machine. *Ciba Found. Symp.* 327–339.

492 Wu, G., van der Helm, F.C.T., Veeger, H.E.J.D., Makhsous, M., Van Roy, P., Anglin, C.,
493 Nagels, J., Karduna, A.R., McQuade, K., Wang, X., Werner, F.W., Buchholz, B.,
494 International Society of Biomechanics, 2005. ISB recommendation on definitions of
495 joint coordinate systems of various joints for the reporting of human joint motion--Part
496 II: shoulder, elbow, wrist and hand. *J Biomech* 38, 981–992.

497 Wu, W., Lee, P.V.S., Bryant, A.L., Galea, M., Ackland, D.C., 2016. Subject-specific
498 musculoskeletal modeling in the evaluation of shoulder muscle and joint function. *J.*
499 *Biomech.* 49, 3626–3634. <https://doi.org/10.1016/j.jbiomech.2016.09.025>

500 Yanagawa, T., Goodwin, C.J., Shelburne, K.B., Giphart, J.E., Torry, M.R., Pandy, M.G., 2008.
501 Contributions of the Individual Muscles of the Shoulder to Glenohumeral Joint Stability
502 During Abduction. *J Biomech Eng* 130. <https://doi.org/10.1115/1.2903422>

503 Yang, C., Leitkam, S., Côté, J.N., 2019. Effects of different fatigue locations on upper body
504 kinematics and inter-joint coordination in a repetitive pointing task. PLOS ONE 14,
505 e0227247. <https://doi.org/10.1371/journal.pone.0227247>
506